

1 **Simulating wind characteristics through direct optimization**

2 **procedures: illustration with three Russian sites**

3 Aleksei Kangash^a, Muhammad Shakeel Virk^b, Pavel Maryandyshev^a, **Alain Brillard**^{1a,c}

4
5 ^a *Northern (Arctic) Federal University, naberezhnaya Severnoy Dviny 17, 1632002, Arkhangelsk,*
6 *Russia*

7 ^b *UiT The Arctic University of Norway, Lodve Langes Gate 2, 8515 Narvik, Norway*

8 ^c *University of Haute-Alsace, Laboratoire Gestion des Risques et Environnement, 3bis rue Alfred*
9 *Werner, 68093 Mulhouse, France*

10 *Email: p.marjyandishev@narfu.ru

11 **Abstract**

12 Wind energy assessment of a territory where a wind park is planned to be built is important. This can
13 be performed through an appropriate evaluation of the wind characteristics in this territory. To
14 simulate the wind speeds, a Weibull function is recommended whose parameters are classically
15 determined either applying logarithms or using one of the formulas proposed in the literature. In the
16 present study, direct optimization procedures are applied, which consist to minimize the squared
17 difference between the experimental and simulated densities or probabilities. These procedures are
18 applied on the wind characteristics collected from the ERA5 website during forty-one years at three
19 Russian sites close to Arkhangelsk. These direct optimization procedures are proved to give lower
20 errors than the classical one or the formulas of the literature. They also lead to lower values of the
21 estimated Annual Energy Production for a Vestas V90-2.0 wind turbine. Direct optimization
22

¹ Corresponding author. Alain Brillard
Email: alain.brillard@uha.fr
<https://orcid.org/0000-0003-0615-8880>

University of Mulhouse, Lab. Gestion des Risques et Environnement, 3bis rue Alfred Werner, 68093 Mulhouse, France
Northern (Arctic) Federal University, naberezhnaya Severnoy Dviny 17, Arkhangelsk, Russia

23 procedures are also applied to determine the optimal parameters associated with a unique or a
24 superposition of two von Mises distribution functions to simulate the wind directions in these three
25 Russian sites.

26

27 **Keywords.** Wind characteristics; Weibull distribution function; von Mises distribution function;
28 Direct optimization procedure; Optimal parameters

29

30 **1. Introduction**

31 The continuous development of the world economies leads to an increasing energy consumption.
32 Fossil energy sources still account for the major part in the energy balance of many countries
33 throughout the world. This highly affects the climate and environmental changes observed and
34 described by scientists around the world. The use of fossil fuels for energy production indeed causes
35 the formation and release into the atmosphere of hazardous substances such as sulfur, nitrogen and
36 carbon oxides, as well as particulate matter. Carbon dioxide is one of the main gases that contribute
37 to the greenhouse effect. Compounds of substances that are released into the atmosphere by
38 combustion of fossil fuels can have a serious impact on human health and wildlife. In northern
39 countries, the difficulty of delivering fossil fuel here increases its cost several times. There is a further
40 risk of spills during transportation. In addition, fossil fuel power plants produce large amounts of
41 pollutants as well as noise emissions. Considering these disadvantages, the use of large quantities of
42 fossil fuels is unsustainable in remote northern territories. These issues make the use of renewable
43 energy sources a priority for many countries throughout the world. The use of environmentally
44 friendly natural renewable energy sources can provide effective, sustainable and safe energy
45 production. Renewable energy sources have almost no significant impact on the environment, when
46 compared to fossil sources and are available in large amounts in many regions of the world, even if
47 they are non-permanent sources.

48 Wind energy is one of the main renewable sources. Wind energy industry has strengthened its position
49 in the electricity production throughout the world in the recent years. In some countries, wind power
50 plays an important role in the balance of power generation. More and more new wind parks are being
51 built in the world every year. However, at the moment it is difficult to replace fossil fuels with wind
52 power everywhere. Therefore, scientific research and new technical developments that can increase
53 the efficiency of wind energy usage are needed.

54 Estimating the wind energy potential of the territory where a wind park is planned to be built is very
55 important. A preliminary estimation based on available data concerning the wind characteristics and
56 a forecast of these characteristics in a reasonable future can give an idea of whether the location of
57 the wind park in this area will be efficient and how much energy can be generated by its installation.

58 An important parameter of a wind park project is its Annual Energy Production (AEP). This
59 parameter can be increased with a correct location of wind turbines. An inaccurate assessment of the
60 wind energy resources of the area, as well as an incorrect location of the planned wind turbines can
61 cause inefficient production from the wind farm. The energy production will be less than planned and
62 this situation may lead to significant economic losses. Wind resource assessment of the territory is
63 very important for areas where no wind parks were constructed before. Therefore, each territory
64 requires appropriate studies before installation of a wind park. Wind resource assessment can
65 contribute to the successful implementation of a wind park project and prevent from fatal mistakes at
66 the design stage. Northern areas have high wind energy potential [1–3].

67 In the present study, a Vestas V90-2.0 wind turbine is intended to be located in three Russian sites:
68 Dolgoshchelye (lat. 66.3, long. 43.3), hereafter called in short Dolgo, Mezen (lat. 62.4, long. 38.5)
69 and Solovetsky Islands (lat. 65.7, long. 35.4), hereafter called Solov. The wind directions and speeds
70 were collected over forty-one years at the altitude of 100 m from ERA5 site [4]. Simulations of the
71 wind speeds using a Weibull function were performed through different formulas or procedures
72 already proposed in the literature, [5,6], for example. Direct optimization procedures were also
73 applied which allow determining the optimal parameters of a Weibull distribution function. These

74 direct optimization procedures avoid the use of the logarithm which overrides the variations of the
75 data to be considered. The simulations returned by these direct optimization procedures are compared
76 with that returned using a classical procedure or formulas of the literature. To validate the values of
77 the parameters, different error formulas are used. The differences between the values of the
78 parameters have a significant impact on the wind potential of a site, as evaluated for example through
79 the Annual Energy Potential. Direct optimization procedures are also applied to simulate the wind
80 directions, considering a unique or the superposition of two von Mises distribution functions.

81

82 2. Material and Methods

83 2.1. Characteristics of the Russian sites and of the Vestas V90 wind turbine

84 The behavior of a Vestas V90-2.0 wind turbine to be located in three Russian sites is investigated.
85 The three sites are located in the Arkhangelsk region (oblast), northwest of the Russian Federation,
86 see Fig. 1 a).



a)



b)



c)

87

88 **Fig. 1.** Position of the three Russian sites in the Arkhangelsk region a), and photos of the Mezen b)
89 and Solovetsky Islands c).

90

91 The sites where the wind turbine is intended to be placed are almost flat and do not present irregular
92 obstacles, see Fig. 1 b) and c). The Dolgoshchelye site is located around a small village in the tundra.
93 For the Dolgoshchelye site, the maximal and minimal wind speeds are respectively equal to 14.61
94 and 0.91 m/s, respectively. For the Mezen site, the maximal and minimal wind speeds are respectively
95 equal to 14.16 and 0.85 m/s, respectively, quite comparable to that of the Dolgoshchelye site. For the
96 Solovetsky Islands site, the maximal and minimal wind speeds are respectively equal to 20.76 and
97 0.84 m/s, respectively, the maximal wind of this last site being much higher than the maximal values
98 for the two other sites. In the three cases, the wind directions cover almost the whole range 0-360°.
99 More detailed statistical analyses of the wind speeds and directions in the three sites are given in
100 section 3.1.

101 The Vestas V90-2.0 wind turbine to be installed in the three sites has a rated power equal to 2 kW
102 [7]. Its hub height is 80 m. More details concerning this wind turbine are given in section 3.2.3.

103

104 **2.2. Wind characteristics**

105 Wind characteristics were collected from the ERA5 website [4], at the altitude of 100 m and each
106 hour during forty-one years (1979-2020). The Windographer software was used to collect the data.
107 Because of the huge number of data (368,184), daily means were first computed to reduce the number
108 of data to 15,341.

109

110 **2.3. Analysis of wind data and determination of the main parameters**

111 **2.3.1. Simulation of the wind speeds distribution through a Weibull distribution function** 112 **using the classical procedure**

113 Concerning the wind speed, a two-parameters Weibull distribution function is recommended by the
114 standards IEC 61400-12-1:2017 [8], to assess the values of the wind speed according to their
115 frequency. The density of the Weibull function is written as:

$$116 \quad f_W(v) = \frac{k}{c} \left(\frac{v}{c}\right)^{k-1} \exp\left(-\left(\frac{v}{c}\right)^k\right), \quad (1)$$

117 where k is the dimensionless shape parameter and c (m/s) is the scale parameter. The cumulative
118 distribution function of this Weibull function is:

$$119 \quad W(v) = 1 - \exp\left(-\left(\frac{v}{c}\right)^k\right). \quad (2)$$

120 To determine the two parameters in the present context, the daily mean wind speeds are first ordered
121 in an increasing way. Then a frequency is associated with each daily mean speed, according to the
122 two following possibilities:

- 123 - Either a constant frequency equal to $1/(n_d + 1)$ to each daily speed, where $n_d = 15,341$ is
124 the number of observed daily mean speeds in the present study,
- 125 - Or the daily mean speeds are assembled in n_c classes, for example according to Brook-
126 Carruthers' formula:

$$127 \quad n_c = 5 \times \log_{10}(n_d), \quad (3)$$

128 a constant frequency equal to $\#j/(n_c + 1)$ is here associated with each daily mean speed in
 129 the class j , where $\#j$ is the number of daily mean speeds in the class j .

130 In the present study, only the second method will be used.

131 Cumulative probabilities are then deduced from these frequencies.

132 Because of the structure (2) of the Weibull function, a classical attempt to determine the shape and
 133 scale parameters of the Weibull function consists to apply twice the natural logarithm to (2):

$$134 \quad \ln(-\ln(1 - W(v))) = k\ln(v) - k\ln(c). \quad (4)$$

135 A linear regression method is then used to determine the values of k and $k\ln(c)$, whence of c . This
 136 procedure will be called the classical method. This procedure uses the logarithm which is known to
 137 override the variations of the data. This quite simple procedure does not require any numerical
 138 software.

139

140 **2.3.2. Simulation of the wind speeds distribution through a Weibull distribution function** 141 **using direct optimization procedures**

142 The shape and scale parameters of a Weibull function simulating the density or probability of wind
 143 speed in some territory can be derived minimizing the square root of the squared differences between
 144 the observed $f_{i,obs}$ and simulated frequencies:

$$145 \quad l_f^2 = \left(\sum_{i=1}^{n_d} \left(f_{i,obs} - \frac{k}{c} \left(\frac{v_i}{c} \right)^{k-1} \exp \left(- \left(\frac{v_i}{c} \right)^k \right) \right)^2 \right)^{1/2}, \quad (5)$$

146 or between the observed $W_{i,obs}$ and simulated cumulative probabilities:

$$147 \quad l_p^2 = \left(\sum_{i=1}^{n_d} \left(W_{i,obs} - 1 + \exp \left(- \left(\frac{v_i}{c} \right)^k \right) \right)^2 \right)^{1/2}, \quad (6)$$

148 In the present study, the Scilab software and especially its routine ‘datafit’ is used to determine the
 149 optimal values of the shape and scale parameters. This Scilab ‘datafit’ routine uses the quasi-Newton
 150 algorithm.

151 When considering the objective function defined in (5) based on the observed and simulated
 152 frequencies, the optimization procedure will be called Directf. When considering the objective
 153 function defined in (6) based on the observed and simulated probabilities, the optimization procedure
 154 will be called Directp.

155

156 **2.3.3. Simulation of the wind speeds distribution through a Weibull distribution function** 157 **using other models or formulas**

158 Other methods or formulas have already been proposed in the literature to derive the shape and scale
 159 parameters of a Weibull function which simulates the wind speeds in a territory, see for example [9]
 160 and the references therein. For example, direct computations may be applied such as:

161 - *Modified maximum likelihood*

162 The shape parameter k is determined through the resolution of the nonlinear equation:

$$163 \quad k = \left(\frac{\sum_{i=1}^{n_d} v_i^k \ln(v_i) f_{i,obs}}{\sum_{i=1}^{n_d} v_i^k f_{i,obs}} - \frac{\sum_{i=1}^{n_d} \ln(v_i)}{n_d} \right)^{-1}, \quad (7)$$

164 which is solved in the present study using the Scilab routine ‘fsolve’. The scale parameter is
 165 then computed as:

$$166 \quad c = \left(\sum_{i=1}^{n_d} v_i^k f_{i,obs} \right)^{1/k}. \quad (8)$$

167 - *Lysen*

168 The shape and scale parameters are computed through:

$$169 \quad k = \left(\frac{\sigma}{\bar{v}} \right)^{-1.086}; \quad c = \bar{v} \left(0.58 + \frac{0.433}{k} \right)^{-1/k}, \quad (9)$$

170 where σ is the standard deviations of the wind speeds and $\bar{v} = \sum_{i=1}^{n_d} v_i / n_d$ their mean.

171 - *Energy pattern factor or Justus*

172 The shape and scale parameters are computed through:

$$173 \quad k = 1 + \frac{3.69}{(E_{pfm})^2}; c = \frac{v_{av}}{\Gamma\left(1 + \frac{1}{k}\right)}, \quad (10)$$

174 where Γ is the Gamma function and:

$$175 \quad E_{pfm} = \frac{\sum_{i=1}^{n_d} v_i^3}{n_d(\bar{v})^3}. \quad (11)$$

176 - *Moments*

177 The shape and scale parameters are computed through:

$$178 \quad k = \left(0.9874 \times \frac{\bar{v}}{\sigma}\right)^{1.0983}; c = \frac{\bar{v}}{\Gamma\left(1 + \frac{1}{k}\right)}. \quad (12)$$

179 The values of the shape and scale parameters returned by these methods or formulas will be compared
180 for the three Russian sites, considering the properties of a Vestas V90-2.0 wind turbine.

181 To validate the values of the shape and scale parameters determined through these different
182 procedures or formulas, differences between the observed and simulated frequencies or probabilities
183 are computed through the l_f^2 -norm (5) involving the frequencies or the l_p^2 -norm (6) involving the
184 probabilities. Some authors also introduce a root mean square error (*RMSE*) which is equal to the l^2 -
185 norm, divided by $1/\sqrt{n_d}$. A χ^2 formula is usually computed but which is the square of $RMSE \times$
186 $\sqrt{n_d/(n_d - 2)}$, as there are two parameters to be determined (shape and scale parameters). A R^2
187 formula is also computed which involves the frequencies but which is equal to $1.0 -$
188 $(l_f^2)^2 / \sum_{i=1}^{n_d} (f_{i,obs} - \overline{f_{i,obs}})^2$, where $\overline{f_{i,obs}}$ is the mean value of the observed frequencies. The maximal
189 differences between the observed and simulated frequencies or probabilities hereafter respectively
190 named l_f^∞ - and l_p^∞ -norms, can also be computed. In the present study, only the l_f^2 , and l_p^2 , l_f^∞ , and l_p^∞
191 values will be computed to evaluate the simulations of the wind speeds, obtained through the different
192 procedures or formulas. Inverting Weibull function, the differences between the observed and
193 simulated wind speeds will also be evaluated, when considering the different sets of parameters.

194

195 **2.3.4. Determination of the power density, of the Annual Energy Production, of the**
196 **capacity factor, and of the power output of a wind turbine**

197 The wind power density (W/m^2) is an important parameter to characterize the wind potential of a site.

198 It is defined as:

199
$$P_d = \frac{1}{2} \rho c^3 \Gamma \left(1 + \frac{3}{k} \right), \quad (13)$$

200 where ρ is the air density which will be taken equal to 1.225 kg/m^3 , value corresponding to sea level
201 (1 atm) and under a temperature of $15 \text{ }^\circ\text{C}$. Some authors analyzed the variations of the air density and
202 the impact of this physical parameter on the wind energy assessment, see [10] for example.

203 Values of this power density may be taken per year in the present context. However, a unique value
204 will here be considered for the forty-one years of observations.

205 The theoretical Annual Energy Production (MWh) of the Vestas V90-2.0 wind turbine is computed
206 through:

207
$$AEP = 365 \times 24 \times \int_{v_{ci}}^{v_{co}} P(v) f(v) dv, \quad (14)$$

208 where v_{ci} is the cut-in wind speed (m/s), v_{co} is the cut-off wind speed (m/s), P (kW) is the power
209 output of the wind turbine under consideration, given by the manufacturer [7], P being a function of
210 the wind speed, and f is the Weibull density representing the frequencies of the wind speeds and
211 defined in (1).

212 From this theoretical Annual Energy Production and the rated power P_r of the wind turbine, which is
213 indicated by the manufacturer, it is possible to determine a theoretical capacity factor through:

214
$$C_{f,t} = \frac{AEP}{P_r \times 365 \times 24}. \quad (15)$$

215 The power density P_d , the Annual Energy Production and the capacity factor $C_{f,t}$, respectively defined
216 through (13), (14), and (15), depend on the shape and scale parameters involved in the Weibull

217 distribution function W (2) and its density f (1) which represent the probabilities and densities of the
 218 wind speeds observed in the site under consideration.

219 The power output P of the wind turbine depends on the wind speed and takes different expressions
 220 according to the value of this wind speed with respect to the cut-in wind speed v_{ci} , the rated wind
 221 speed v_r , and the cut-off wind speed v_{co} :

$$222 \quad P(v) = \begin{cases} 0 & \text{if } v < v_{ci} \\ P_f(v) & \text{if } v_{ci} \leq v < v_r \\ P_r & \text{if } v_r \leq v < v_{co} \\ 0 & \text{if } v > v_{co} \end{cases} \quad (16)$$

223 these cut-in, rated, and cut-off wind speeds being defined by the manufacturer website [7].

224 The capacity factor defined in (15) may be expressed in terms of the power output as, [11]:

$$225 \quad C_{f,t} = \frac{\bar{P}}{P_r}; \quad \bar{P} = \int_0^{+\infty} P(v)f(v)dv = \int_{v_{ci}}^{v_r} P_f(v)f(v)dv + P_r \int_{v_r}^{v_{co}} f(v)dv. \quad (17)$$

226 In [12], the authors propose different formulas to estimate the capacity factor of a wind turbine.

227 A sensitivity analysis and a parametric study of the Annual Energy Production will be performed for
 228 the Dolgoshchelye site, with respect to the power output or the density energy.

229

230 **2.3.5. Simulation of the wind distributions through von Mises distribution functions**

231 Usually, simulations of the wind directions are performed considering a unique or the superposition
 232 of two von Mises functions, [11]. The use of a von Mises function first requires the conversion of the
 233 wind distributions in radians. The density of a von Mises function is defined as:

$$234 \quad f_{M,\mu,\kappa}(\theta) = \frac{\exp(\kappa \cos(\theta - \mu))}{2\pi I_0(\kappa)} = \frac{I_0(\kappa) + 2 \sum_{p=1}^{\infty} I_p(\kappa) \cos(p(\theta - \mu))}{2\pi I_0(\kappa)}, \quad (18)$$

235 where θ is the wind distribution (Rad), μ is the shape or a location parameter (Rad), κ is the scale or
 236 concentration parameter (no unit), and I_j is the modified Bessel function of order j . The associated
 237 cumulative probability is given as:

$$238 \quad F_{M,\mu,\kappa}(\theta) = \frac{\theta I_0(\kappa) + 2 \sum_{p=1}^{\infty} I_p(\kappa) (\sin(p(\theta - \mu)) + \sin(p(\mu))) / p}{2\pi I_0(\kappa)}. \quad (19)$$

239 In the case of a superposition of two von Mises distributions, a weight $w \in (0,1)$ is further introduced
 240 and the density of this superposition of two von Mises functions is the weighted sum of the previously
 241 defined densities:

$$\begin{aligned}
 242 \quad & f_{M,\mu_1,\kappa_1,\mu_2,\kappa_2}(\theta) \\
 243 \quad & = w \frac{I_0(\kappa_1) + 2 \sum_{p=1}^{\infty} I_p(\kappa_1) \cos(p(\theta - \mu_1))}{2\pi I_0(\kappa_1)} \\
 244 \quad & + (1 - w) \frac{I_0(\kappa_2) + 2 \sum_{p=1}^{\infty} I_p(\kappa_2) \cos(p(\theta - \mu_2))}{2\pi I_0(\kappa_2)}. \quad (20)
 \end{aligned}$$

245 The cumulative probability associated with this superposition of two von Mises distributions is equal
 246 to:

$$\begin{aligned}
 247 \quad & F_{M,\mu_1,\kappa_1,\mu_2,\kappa_2}(\theta) \\
 248 \quad & = w \frac{\theta I_0(\kappa_1) + 2 \sum_{p=1}^{\infty} I_p(\kappa_1) (\sin(p(\theta - \mu_1)) + \sin(p(\mu_1))) / p}{2\pi I_0(\kappa_1)} \\
 249 \quad & + (1 - w) \frac{\theta I_0(\kappa_2) + 2 \sum_{p=1}^{\infty} I_p(\kappa_2) (\sin(p(\theta - \mu_1)) + \sin(p(\mu_1))) / p}{2\pi I_0(\kappa_2)}. \quad (21)
 \end{aligned}$$

250 In the present study, the wind distributions are first ordered in an increasing way and classified in 20
 251 classes, according to Brook-Carruthers' formula (3). In the present study, the optimal parameters of
 252 a unique or of a superposition of two von Mises function are again determined using the Scilab
 253 software and direct optimization procedures dealing with either the density or the probability. These
 254 procedures are respectively denoted as Directf1, Directp1, Directf2 and Directp2.

255 To validate the simulations performed with these procedures, the l_f^2 - and l_p^2 -norms, as derived from
 256 (5)-(6), and the maximal differences (l_f^∞ - and l_p^∞ -norms) between the observed and simulated
 257 cumulative probabilities will be computed and compared.

258

259 **3. Results and discussion**

260 **3.1. Wind characteristics in the three Russian sites**

261 The mean and standard deviations of the daily mean wind speeds collected from the ERA5 website
 262 during forty-one years for the three Russian sites are gathered in Table 1.

263

264 **Table 1.** Mean and standard deviations of the daily mean speeds and directions for the three Russian
 265 sites.

Site	Wind speed		Wind direction	
	Mean (m/s)	Standard deviations (m/s)	Mean (rad)	Standard deviations (rad)
Dolgo	6.018	2.043	3.340	1.355
Mezen	5.760	1.886	3.393	1.337
Solov	8.561	3.272	3.276	1.337

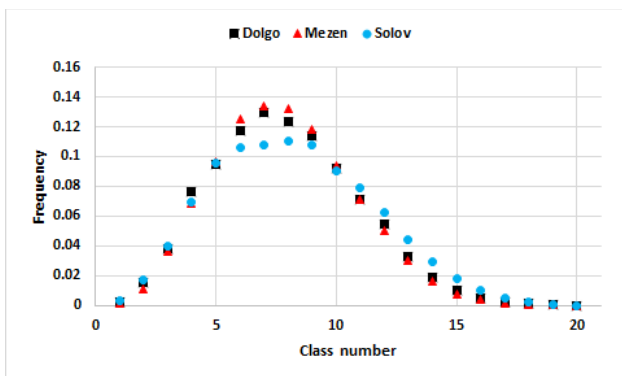
266

267 The mean of the daily mean speeds is much higher in the Solovetsky Islands than in the two other
 268 sites. Its standard deviations is also much higher, which means that the wind speeds here present
 269 larger variations around a higher mean, than in the two other sites. The wind speeds in Mezen present
 270 the lowest mean and standard deviations.

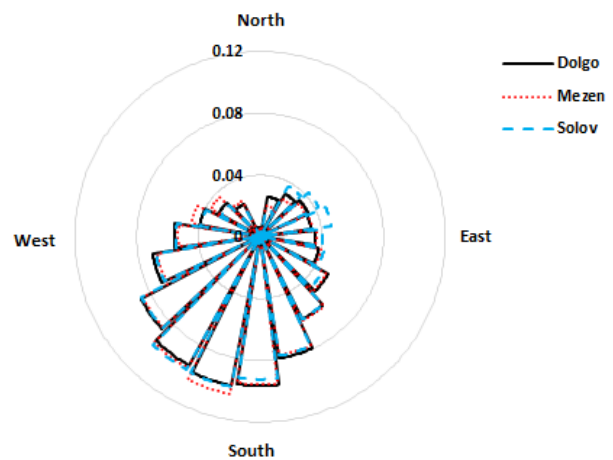
271 The wind directions present quite similar mean and standard deviations for the three sites.

272 According to Brook-Carruthers' formula (3), the collected wind speeds and directions were
 273 assembled into 20 classes. For the wind directions, the first sector is centered around the north. Wind
 274 roses and wind speed distributions are shown in Fig. 2, for the three Russian sites.

275



a)



b)

276 **Fig. 2.** Wind speed frequencies a) and wind direction roses b) for the Russian site Dolgoshchelye
 277 (black squares or solid line), Mezen (red triangle or dotted line) and Solovetsky Islands (blue points
 278 or hyphenated line).

279

280 The wind speed frequencies exhibit small differences between the three sites: the Mezen site presents
 281 slightly higher frequencies around the peak and slightly lower frequencies for the last classes. The
 282 Solovetsky site presents slightly lower frequencies around the peak which occurs here for higher
 283 classes and slightly higher frequencies for the last classes.

284 The wind roses also present small differences between the three sites, in the major or minor directions:
 285 the Solovetsky Islands site presents higher frequencies in the Northeast direction than the two other
 286 sites; the Mezen site presents higher frequencies in the Northwest direction than the two other sites.
 287 For the three sites, the wind mainly blows from the Northwest direction, which confirms the values
 288 of Table 1.

289

290 **3.2.Simulations of the wind characteristics through Weibull functions**

291 **3.2.1. Determination of the shape and scale parameters of the Weibull distribution function** 292 **through the classical procedure**

293 The parameters of a Weibull function which simulates the wind speeds are first determined through
 294 the classical procedure, according to the procedure described in section 2.3.1. The values are gathered
 295 in Table 2 for the three sites, together with the four selected errors.

296

297 **Table 2.** Values of the shape and scale parameters, according to the model described in section 2.3.1,
 298 l_f^2 and l_p^2 errors as defined in (5)-(6), and maximal differences between observed and simulated
 299 frequencies l_f^∞ and probabilities l_p^∞ .

	k	c (m/s)	l_f^2	l_p^2	l_f^∞	l_p^∞
Dolgo	3.133	6.346	1.416	5.173	0.036	0.053

Mezen	3.260	6.058	1.554	5.406	0.035	0.053
Solov	2.710	9.065	1.015	5.149	0.022	0.055

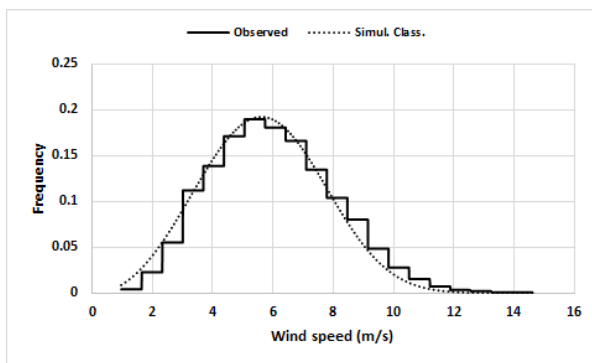
300

301 The values of the shape and scale parameters present high differences between the three sites. The
 302 Solovetsky Islands site has the lowest shape value and the much higher scale value. On the contrary,
 303 the Mezen site has the higher shape value and the lowest scale value. The Dolgoshchelye site presents
 304 intermediate values of the shape and scale parameters.

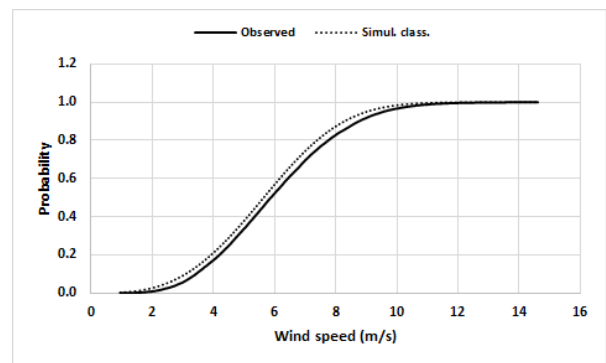
305 The l_f^2 - and l_p^2 -norms (5)-(6) are lower for the Solovetsky Islands site and higher for the Mezen site.
 306 The l_f^∞ -norm is lower for the Solovetsky Islands site and higher for the Dolgoshchelye site. The l_p^∞ -
 307 is slightly higher for the Solovetsky Islands than for the two other sites.

308 The observed and simulated (through the classical procedure) frequencies and probabilities of the
 309 mean wind speeds are gathered in Fig. 3 for the three Russian sites.

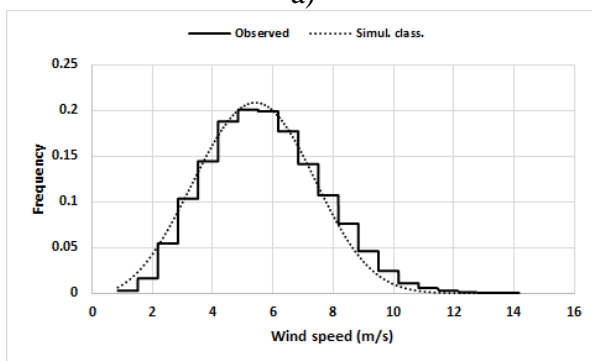
310



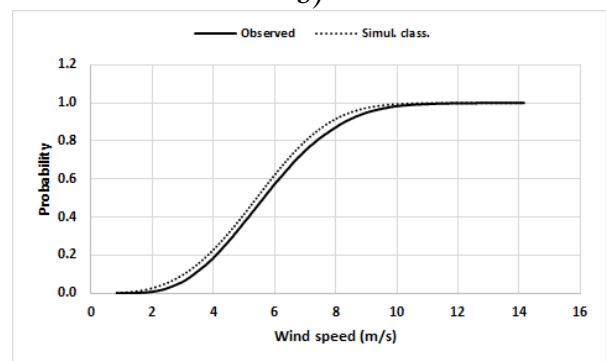
a)



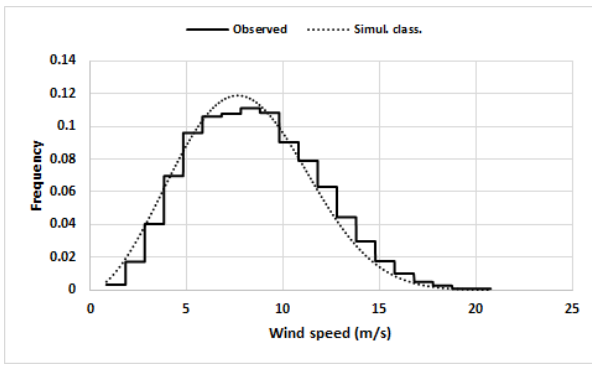
b)



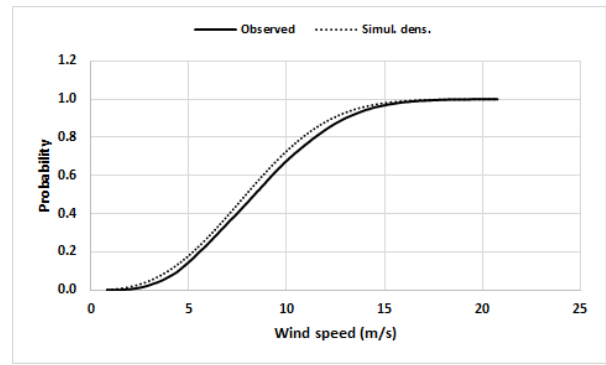
c)



d)



e)



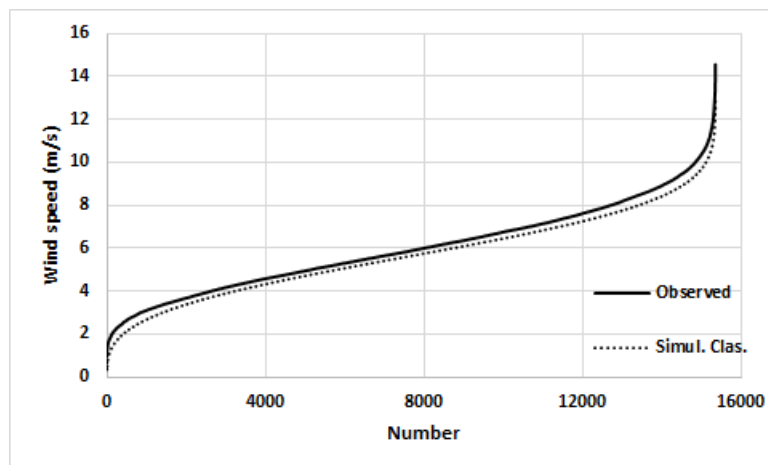
f)

311 **Fig. 3.** Observed (solid line) and simulated (dotted line), with the classical method, densities and
 312 cumulative probabilities of the wind speeds according to a constant frequency in each class of the
 313 20 wind speeds for the Dolgoshchelye (a) and b)), Mezen (c) and d)) and Solovetsky Islands (e) and
 314 f)) sites.

315

316 The density curves present slightly different shapes, while the cumulative probability curves look
 317 similar. Whatever the site, the simulated frequency curve starts above and ends below the observed
 318 one. The probability curve is above the observed one, whatever the site.

319 Inverting the Weibull function (2) with the parameters determined through the classical method, it is
 320 possible to build the wind speeds which correspond to probabilities equal to $(i - 1)/(n_d - 1)$, $i =$
 321 $1, \dots, n_d$, and to measure the differences between the observed and simulated wind speeds. Fig. 4
 322 presents the curves of the observed and simulated wind speeds for the Dolgoshchelye site.



323

324 **Fig. 4.** Observed (solid line) and simulated (dotted line) wind speeds for the Dolgoshchelye site.

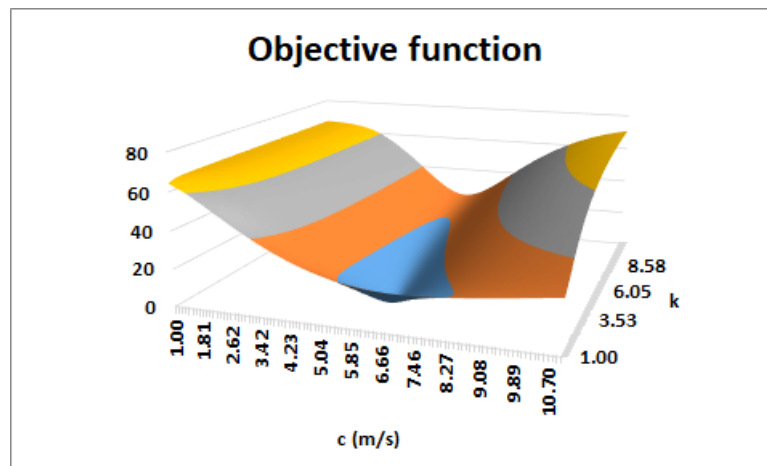
325 The maximal difference between the observed and simulated wind speeds is equal to 1.51 m/s. The
326 l^2 norm of the differences is equal to 45.27 m/s. Similar results can be obtained for the two other
327 sites.

328

329 **3.2.2. Determination of the shape and scale parameters of the Weibull distribution function** 330 **through the direct optimization procedures**

331 When considering the direct optimization procedure applied to the Weibull function, the objective
332 function defined in (6) and to be minimized has the shape presented in Fig. 5, for k and c both varying
333 in the interval $[1,10]$. Here only the Dolgoshchelye site is considered, the other Russian sites leading
334 to quite similar results.

335



336

337 **Fig. 5.** Values of the objective function defined in (6) for k and c both varying in the interval $[1,10]$
338 and for the Dolgoshchelye site.

339

340 This objective function presents a minimum for values of k close to 2 and of c close to 6. This
341 minimizer looks unique. Quite similar observations can be brought for the two other sites (not shown
342 here).

343

344 The values of the shape k and scale c parameters defined through the different models indicated in
 345 the expressions (7)-(12) of section 2.3.3 are also gathered in Table 3.

346

347 **Table 3.** Values of the shape and scale parameters, according to the direct optimization methods
 348 described in sections 2.3.2 and to formulas presented in section 2.3.3, l_f^2 - and l_p^2 -errors as defined in
 349 (5)-(6), and maximal differences between the observed and simulated frequencies (l_f^∞) and
 350 probabilities (l_p^∞).

	Directf	Directp	Max. like.	Lysen	Energy pattern factor (Justus)	Moments
Dolgo						
k	3.089	2.973	3.186	3.232	2.995	3.230
c (m/s)	6.499	6.307	6.723	6.679	6.740	6.740
l_f^2	1.540	1.174	1.608	1.557	1.669	1.714
l_p^2	3.615	4.961	8.080	7.652	7.709	8.469
l_f^∞	0.043	0.032	0.036	0.036	0.031	0.038
l_p^∞	0.069	0.104	0.144	0.139	0.136	0.148
Mezen						
k	3.091	3.219	3.307	3.362	3.075	3.361
c (m/s)	6.016	6.204	6.422	6.381	6.444	6.444
l_f^2	1.721	1.276	1.771	1.712	1.941	1.915
l_p^2	3.818	5.283	8.534	8.124	8.166	9.049
l_f^∞	0.043	0.033	0.038	0.036	0.039	0.039
l_p^∞	0.072	0.111	0.153	0.148	0.144	0.159
Solov						
k	2.574	2.671	2.837	2.842	2.738	2.836
c (m/s)	9.065	9.437	9.621	9.552	9.622	9.622
l_f^2	1.012	0.731	0.944	0.924	0.821	0.943
l_p^2	3.220	5.045	7.106	6.583	6.706	7.111
l_f^∞	0.019	0.026	0.024	0.023	0.022	0.024
l_p^∞	0.058	0.096	0.125	0.121	0.118	0.125

351

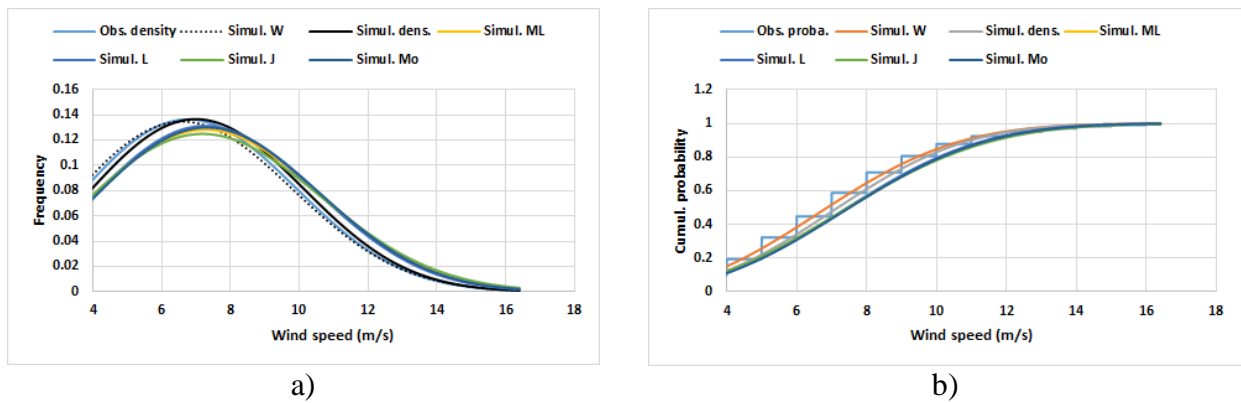
352 Whatever the site, the values of the shape parameter k and of the scale parameter c highly depend of
 353 the method or formula. The Energy pattern factor method returns the lowest values of the shape
 354 parameter k . The Lysen formula returns the highest values of the shape parameter k and scale
 355 parameter c . The direct optimization method Directp (based on the probability) returns the lowest l_f^2 -
 356 error, which is the smallest error among the six methods or formulas, and the highest l_p^2 -error. The

357 direct optimization method Directf (based on the density) returns the lowest l_p^2 -error among the six
 358 methods. The moments formula returns the highest l_f^2 - and l_p^2 -errors.

359 For the Dologoshchelye site, the mean value \bar{k} and the standard deviations σ_k of the k parameters
 360 returned by the different models or formulas are equal to 3.1232 and 0.1151, respectively. The mean
 361 value \bar{c} and the standard deviations σ_c of the c parameters returned by the different models or formula
 362 are equal to 6.6147 and 0.1609 m/s, respectively.

363 The density and cumulative Weibull distributions associated with these six sets of shape and scale
 364 parameters are gathered in Fig. 6.

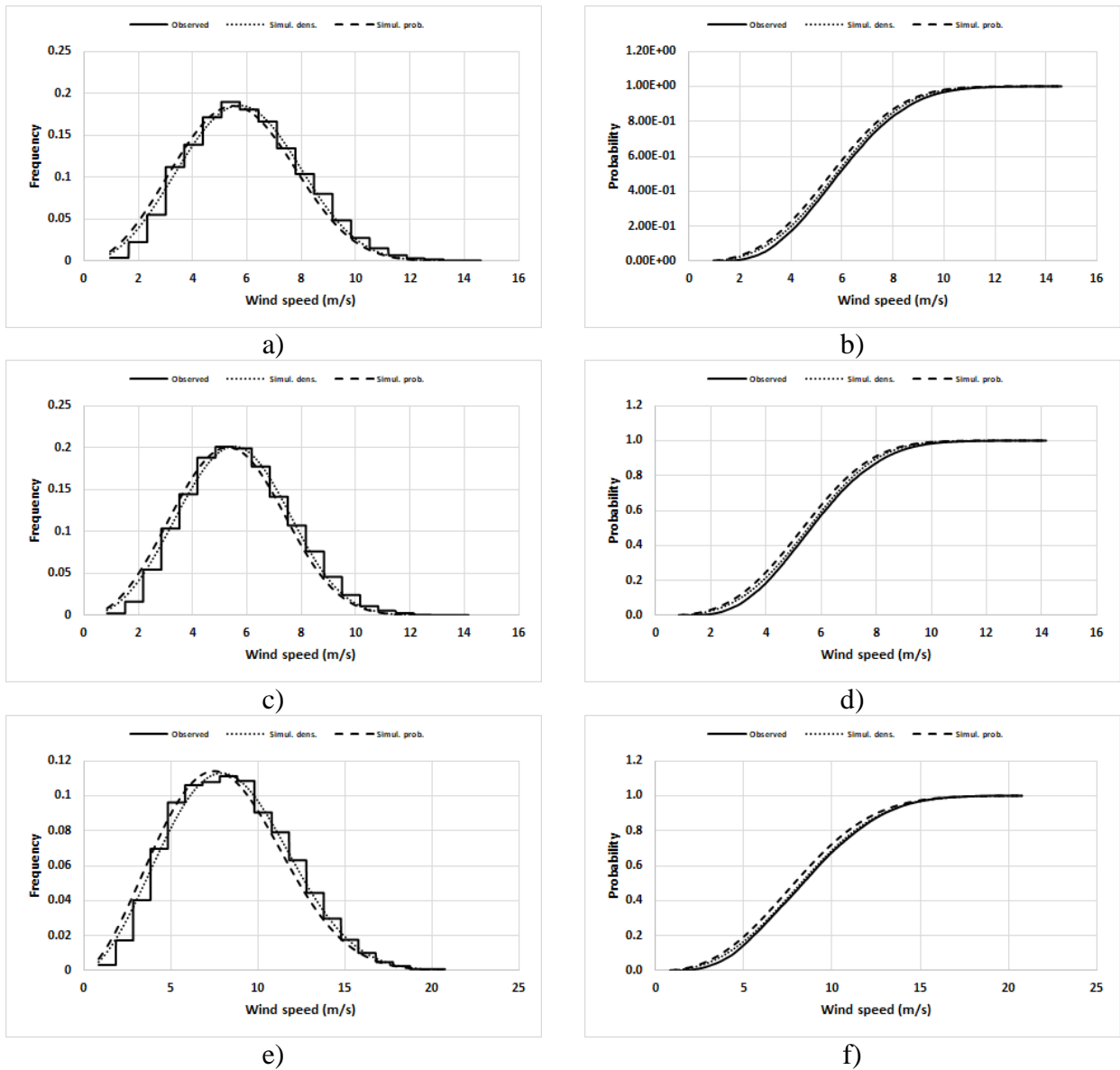
365



366 **Fig. 6.** Observed and simulated density a) and probability b) curves for the Dolgoshchelye site. The
 367 observed curves are in light blue, the simulated curves obtained with the direct optimization with
 368 respect to the probability in red, with the direct optimization with respect to the density in grey,
 369 with maximum likelihood in yellow, Lysen in dark blue, Justus in green, and moments in violet.

370

371 It is difficult to identify the different curves even if they present quite significant differences, see also
 372 Table 3. Figure 7 focuses on the observed and simulated density and probability curves for the three
 373 Russian sites, the simulated curves being obtained with the two direct optimization procedures
 374 described in section 2.3.2.



375 **Fig. 7.** Observed and simulated density and probability curves for the Dolgoshchelye (a) and b)),
 376 Mezen (c) and d)) and Solovetsky Islands sites (e) and f)). The observed curves are the solid lines,
 377 the simulated curves obtained with the direct optimization with respect to the density are the dotted
 378 lines, with the direct optimization with respect to the density are the hyphened lines.
 379
 380 For the three sites, the probability curves seem to be better simulated when considering the direct
 381 optimization curves involving the densities. Whatever the site, the density curves indeed go more
 382 between the steps of the observed density curves when considering the direct optimization curves
 383 involving the densities, especially after the peak.

384 The simulations of the wind speeds presented in this section were based on observations performed
385 at 100 m height, although the hub height of the Vestas V90-2.0 is 85 m. Corrections should be brought
386 to these observed wind speeds, according to a formula given in the literature when considering a quite
387 flat territory, see [12,13], for example.

388 From the Weibull functions whose parameters are determined through the direct optimization
389 methods presented in section 2.3.2, it is possible to build the wind speeds which correspond to
390 probabilities equal to $(i - 1)/(n_d - 1)$, $i = 1, \dots, n_d$, and to measure the differences between the
391 observed and simulated wind speeds. The maximal differences between the observed and simulated
392 wind speeds are equal to 1.14 and 1.09 m/s, when considering the frequencies or probabilities,
393 respectively. These maximal differences are slightly lower than that (1.51 m/s) obtained when
394 considering the Weibull function whose parameters are determined through the classical method. The
395 l^2 -norms of the differences between the observed and simulated wind speeds are equal to 49.56 and
396 29.47 m/s, respectively. The l^2 -norm of the differences between the observed and simulated wind
397 speeds obtained when considering the Weibull function with parameters deduced from the classical
398 method was computed at 45.27 m/s, between the two l^2 -norms.

399

400 **3.2.3. Determination of the power density, AEP and capacity factor**

401 For a Vestas V90-2.0 wind turbine, the cut-in wind speed v_{ci} is equal to 3.0 m/s, the rated wind speed
402 v_r is equal to 12.5 m/s, and the cut-off wind speed v_{co} is equal to 20.5 m/s. The rated power P_r is
403 equal to 2 MW. In the interval $[v_{ci}, v_r]$, the power output P_f (MW) of the wind turbine may be
404 approximated through the polynomial function of degree 6:

$$405 \quad P_f(v) \sim 2.4925 \times 10^{-5} \times v^6 - 1.1420 \times 10^{-3} \times v^5 + 2.0165 \times 10^{-2} \times v^4 - 0.1762 \times v^3 \\ 406 \quad + 0.8298 \times v^2 - 1.9213 \times v + 1.6817. \quad (22)$$

407 The determination coefficient of this polynomial function of degree 6 is higher than 0.999.

408 As deduced from the formulas (13)-(15) in section 2.3.4 and of the values of the scale and shape
 409 parameters determined in the previous section, the values of the power density, of the annual energy
 410 production and of the capacity factor are gathered in Table 4.

411

412 **Table 4.** Values of the power density P_d , of the Annual Energy Production AEP and of the capacity
 413 factor C_f , as deduced from the Weibull functions indicated in Table 3, through the expressions (13)-
 414 (15).

	Directf	Directp	Max. like.	Lysen	Energy pattern factor	Moments
Dolgo						
P_d (W/m ²)	137.2	150.3	166.7	163.5	167.4	168.0
AEP (MWh)	3695.2	3983.5	4352.4	4262.2	4436.8	4371.6
C_f (%)	0.211	0.227	0.248	0.243	0.253	0.250
Mezen						
P_d (W/m ²)	119.2	131.1	145.5	142.9	146.5	147.1
AEP (MWh)	3179.8	3447.6	3790.9	3707.7	3892.8	3814.7
C_f (%)	0.181	0.197	0.216	0.212	0.222	0.218
Solov						
P_d (W/m ²)	405.1	457.6	485.9	475.6	485.4	486.0
AEP (MWh)	8454.5	9060.4	9439.3	9340.8	9373.1	9440.3
C_f (%)	0.483	0.517	0.539	0.533	0.535	0.539

415

416 The power density, Annual Energy Production and capacity factor highly depend on the model. The
 417 direct optimization method based on the density returns the lowest values of the power density, of the
 418 Annual Energy Production and of the capacity factor, whatever the site. The Energy pattern factor
 419 and moments methods return the highest values of these parameters. Concerning the Annual Energy
 420 Production, the relative increase between the lowest and highest values is equal to 20.0% for
 421 Dolgoshchelye, to 22.4% for Mezen and to 11.7% for Solovetsky Islands sites, which are very high
 422 percentages.

423

424 **3.2.4. Sensitivity analysis and parametric study concerning the Annual Energy Production**
 425 **in the case of the Dolgoshchlye site**

426 The formula (14) giving the Annual Energy Production involves the power output, the cut-in v_{ci} and
 427 cut-off v_{co} rates of the wind turbine, as indicated by the manufacturer. The cut-in and cut-off rates
 428 are fixed by the manufacturer, as they deal with efficiency or security reasons. Consequently, the
 429 uncertainty of the Annual Energy Production comes from that of the power out curve or of the Weibull
 430 function. A sensitivity analysis is performed on these two terms, but in an additive way, the case of a
 431 multiplicative uncertainty being indeed trivial. In the case of additive uncertainties on the power
 432 $\delta P(v)$ and on the Weibull density $\delta f(v)$, the uncertainty on the Annual Energy Production is
 433 computed through:

$$\begin{aligned}
 434 \quad AEP + \delta AEP &= 365 \times 24 \int_{v_{ci}}^{v_{co}} (P(v) + \delta P(v))(f(v) + \delta f(v))dv \\
 435 \quad &= 365 \times 24 \int_{v_{ci}}^{v_{co}} (P(v)f(v) + \delta P(v)f(v) + P(v)\delta f(v) + \delta P(v)\delta f(v))dv. \quad (23)
 \end{aligned}$$

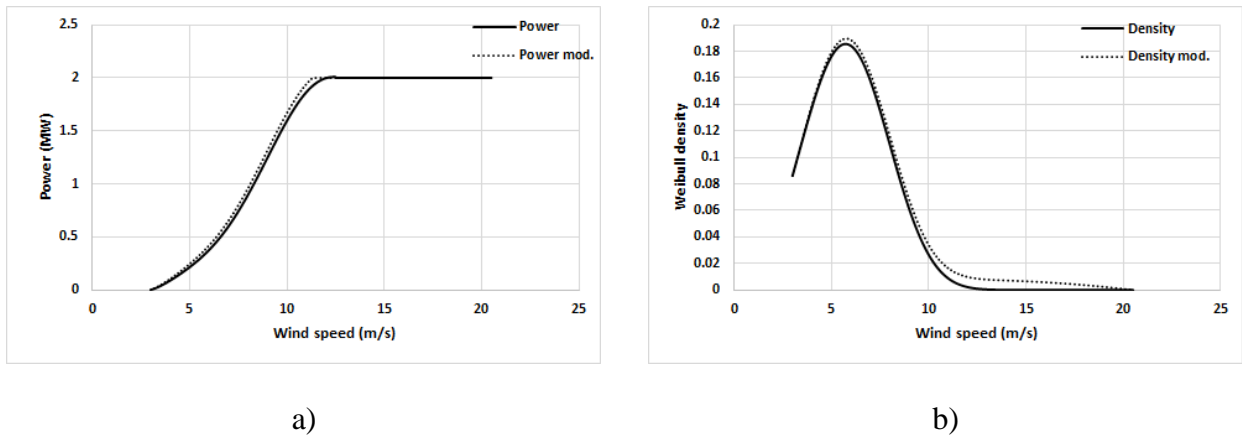
436 The power curve given in (17) was slightly modified through the formula:

$$437 \quad P_{fm}(v) = \max \left(\min \left(P_f(v) - \frac{(v - v_{ci})(v - v_{co})}{1000.0}, P_f(v_{co}) \right), 0.0 \right). \quad (24)$$

438 The Weibull density given in (1) and determined through the direct optimization method with the
 439 probabilities, leading to the values $k = 2.973, c = 6.307$ m/s, see Table 3, was modified according
 440 to the formula:

$$441 \quad f_{Wm}(v) = f_W(v) - \frac{(v - v_{ci})(v - v_{co})}{10000.0}. \quad (25)$$

442 The curves of the original and modified power outputs and densities are gathered in Fig. 8.



443 **Fig. 8.** Original (solid line) and modified (dotted line) power output and density in the interval
 444 $[v_{ci}, v_{co}]$.

445

446 The integral of the absolute difference between the power curves is equal to 0.44 MW, to be compared
 447 to the integral of the power output, which is equal to 24.90 MW, thus representing a relative variation
 448 of 1.7%. The integral of the absolute difference between the density curves is equal to 0.089, to be
 449 compared to the integral of the density which is equal to 1.0, thus representing a relative variation of
 450 8.9%.

451 Only modifying the power output according to (24), the Annual Energy Production increases from
 452 3983.5 to 4317.1 MW, which represents a relative variation of 8.4%. Only modifying the density
 453 according to (25), the Annual Energy Production decreases from 3983.5 to 3943.6 MW, which
 454 represents a relative variation of 1%. Modifying the power output and density expressions, the Annual
 455 Energy Production increases from 3983.5 to 5557.9 MW, which represents a relative variation of
 456 39.5%! Even if the relative variation of the power output is lower than that of the density, its impact
 457 on the variation of the Annual Energy Production is much higher, due to the expression of the integral
 458 leading to the Annual Energy Production.

459 Considering the Dolgoshchelye site, a parametric analysis with respect to the k and c parameters of a
 460 Weibull function can be performed on the Annual Energy Production, taking the five values (\bar{k}, \bar{c})

461 and $(\bar{k} \pm \sigma_k, \bar{c} \pm \sigma_c)$. The values of the Annual Energy Production obtained for these four last values
 462 are gathered in Table 5.

463

464 **Table 5.** Values of the Annual Energy Production for the five values (\bar{k}, \bar{c}) and $(\bar{k} \pm \sigma_k, \bar{c} \pm \sigma_c)$, and
 465 relative variations with respect to the value of the Annual Energy Production obtained when taking
 466 (\bar{k}, \bar{c}) and equal to 4176.8 MWh, third line), and also with respect to the mean value of the Annual
 467 Energy Productions determined through the different methods (Table 4) and equal to 4183.6 MWh,
 468 fourth line).

	(\bar{k}, \bar{c})	$(\bar{k} + \sigma_k, \bar{c})$	$(\bar{k} - \sigma_k, \bar{c})$	$(\bar{k}, \bar{c} + \sigma_c)$	$(\bar{k}, \bar{c} - \sigma_c)$
AEP (MWh)	4176.8	4143.1	4208.8	4464.3	3895.8
		0.81%	0.76%	6.88%	6.73%
	0.16%	0.97%	0.60%	6.71%	6.88%

469

470 Variations of the k parameter approximately equal to 3.7% do not highly modify so much the Annual
 471 Energy Production (relative variations less than 1%). On the contrary, variations of the c parameter
 472 approximately equal to 2.6% significantly modify the Annual Energy Production (variations greater
 473 than 6%).

474 From the values of the parameters presented in Table 4, it is possible to perform an economic analysis
 475 of the wind turbine, like in [14], for example.

476

477 3.2.5. Simulations of the wind directions with a superposition of two von Mises functions

478 The wind distributions obtained from the ERA5 website [4] during forty-one years, converted in
 479 radians and gathered in 20 classes lead to the observed density and probability curves presented in
 480 Fig. 9.

481

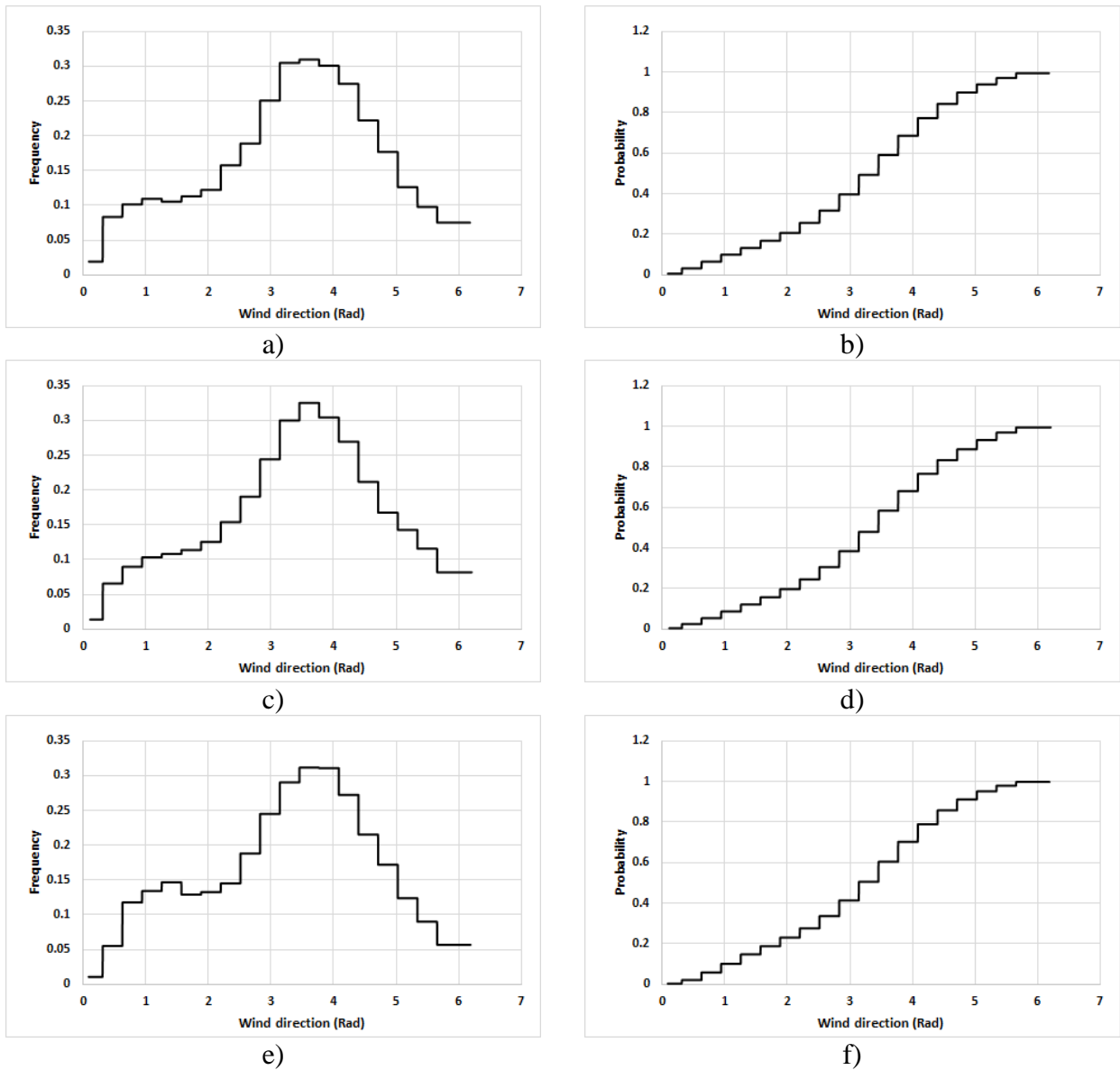


Fig. 9. Observed density and cumulative probability curves of the wind directions for the Dolgoshchelye (a) and b)), Mezen (c) and d)) and Solovetsky (e) and f)) sites.

482
483
484

485 Clearly, two peaks appear on the density curve Fig. 9 a), c) and e), which correspond to the wind rose
486 given in Fig. 2 a), dotted line, the second one being more important and corresponding to winds
487 oriented Southwest.

488 The optimal values of the parameters involved in the unique or in the superposition of two von Mises
489 functions which intend to simulate the wind densities and probabilities directions, according to the
490 direct optimization procedures described in section 2.3.5 are gathered in Table 4. The different errors
491 between the observed and simulated density and probability curves are also gathered in Table 6.

492

493 **Table 6.** Values of the parameters of a unique or of a superposition of two von Mises to simulate the
 494 wind directions, according to the model described in section 2.3.5, l_f^2 - and l_p^2 -errors as adapted in (5)-
 495 (6), and maximal differences between the frequencies l_f^∞ and probabilities l_p^∞ .

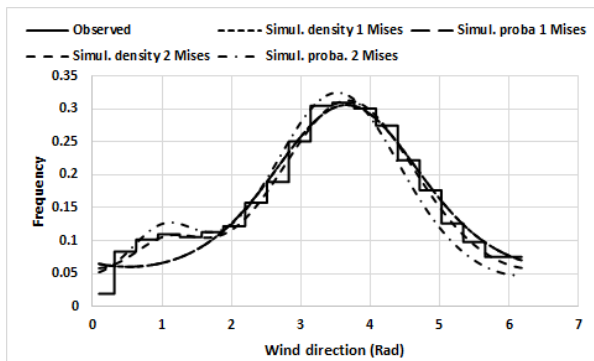
	Directf1	Directp1	Directf2	Directp2
Dolgo				
μ (Rad)	3.661	3.661	-	-
κ (Rad)	0.813	0.813	-	-
μ_1 (Rad)	-	-	1.064	1.021
μ_2 (Rad)	-	-	3.683	3.527
κ_1 (Rad)	-	-	4.205	4.284
κ_1 (Rad)	-	-	0.974	1.107
w	-	-	0.071	0.103
l_f^2	2.259	2.259	1.512	2.259
l_p^2	7.602	7.602	5.345	2.594
l_f^∞	0.046	0.046	0.045	0.046
l_p^∞	0.121	0.121	0.102	0.052
Mezen				
μ (Rad)	3.666	3.666	-	-
κ (Rad)	0.825	0.825	-	-
μ_1 (Rad)	-	-	1.187	1.111
μ_2 (Rad)	-	-	3.690	3.537
κ_1 (Rad)	-	-	4.335	4.740
κ_1 (Rad)	-	-	0.967	1.061
w	-	-	0.063	0.082
l_f^2	2.208	2.208	1.654	2.208
l_p^2	6.732	6.732	4.858	2.618
l_f^∞	0.050	0.050	0.044	0.050
l_p^∞	0.116	0.116	0.099	0.054
Solov				
μ (Rad)	3.648	3.648	-	-
κ (Rad)	0.778	0.778	-	-
μ_1 (Rad)	-	-	1.244	1.170
μ_2 (Rad)	-	-	3.705	3.550
κ_1 (Rad)	-	-	4.289	4.022
κ_1 (Rad)	-	-	1.082	1.232
w	-	-	0.121	0.151
l_f^2	3.392	3.392	1.506	3.392
l_p^2	8.902	8.902	5.337	2.590
l_f^∞	0.069	0.069	0.044	0.069
l_p^∞	0.133	0.133	0.102	0.052

496

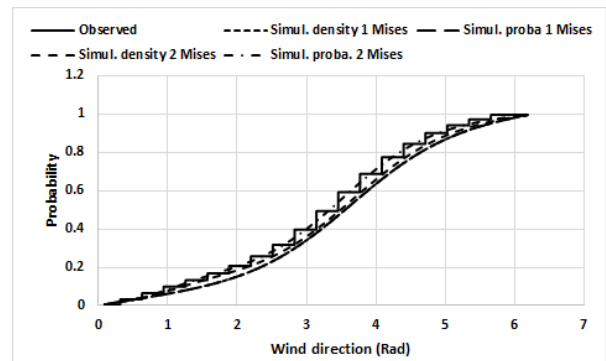
497 Whatever the site and considering a unique von Mises function, the optimal values of the parameters
 498 determined through the two direct optimization procedures are exactly the same. In the case of the
 499 superposition of two von Mises functions, slight differences appear between the two sets of optimal
 500 values. In both cases, the l_f^2 and l_f^∞ errors are smaller when considering the direct optimization
 501 procedure involving the densities. The l_p^2 and l_p^∞ errors are also smaller when considering the direct
 502 optimization procedure involving the probabilities.

503 Figure 10 gathers the observed and simulated density and probability curves for the wind directions
 504 in the three sites.

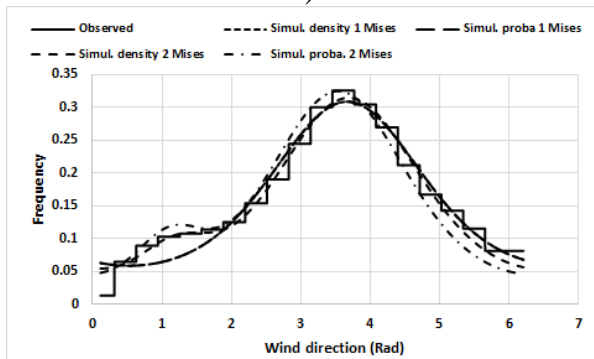
505



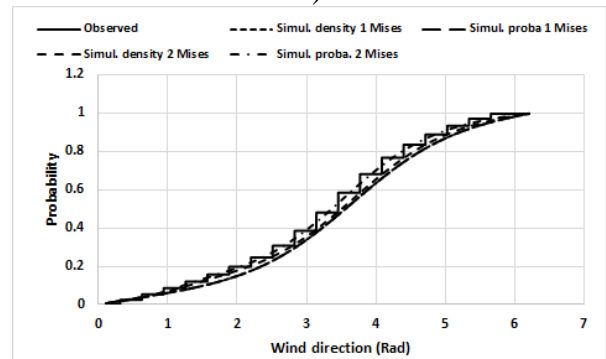
a)



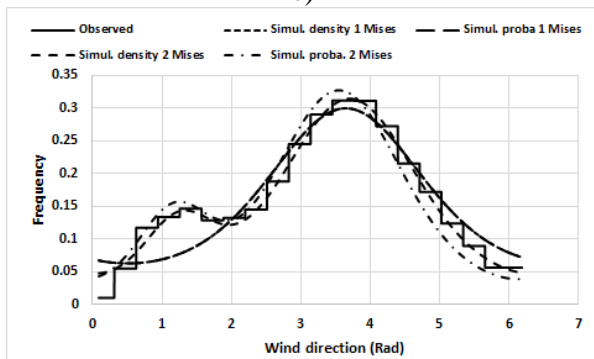
b)



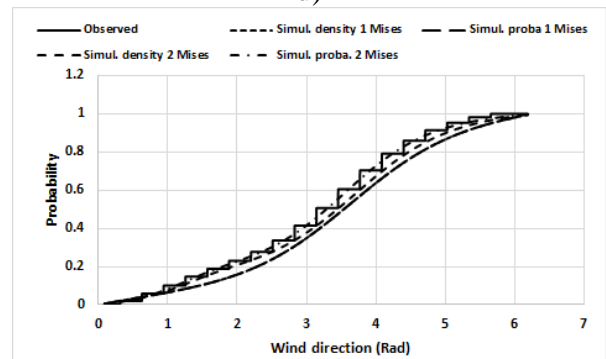
c)



d)



e)



f)

506 **Fig. 10.** Observed (solid line) and simulated with a unique von Mises (dotted line), or with a
507 superposition of two von Mises (hyphenated line) distributions, for the density and cumulative
508 probability of wind directions and for the Dolgoshchelye (a) and b)), Mezen (c) and d)) and
509 Solovetsky (e) and f)) sites.

510

511 The simulations with a unique von Mises function are much poorer than that with a superposition of
512 two von Mises functions. This is the consequence of two peaks, even if the first is much smaller than
513 the second one. Clearly, the simulations with the superposition of the two von Mises distributions
514 with the weight w better reproduce the two peaks and the shape of the observed cumulative
515 probability.

516 Considering the superposition of two von Mises functions, the l_f^2 and l_p^2 errors are quite large,
517 whatever the direct optimization procedure. This is surely the consequence of the shape of the
518 observed density and probability curves. Quite important jumps indeed appear for the lowest values
519 of the wind direction.

520

521 **4. Conclusion**

522 Predicting the power delivered by a wind turbine is important, at least from an economic point of
523 view. Such prediction can be realized analyzing the wind characteristics in the chosen site, simulating
524 them with appropriate tools and taking into account the chosen wind turbine. In the present study, the
525 characteristics of wind data collected from the ERA5 website during forty-one years and concerning
526 three Russian sites in the Arkhangelsk region were analyzed. Concerning the wind speeds, different
527 mathematical methods or formulas, among which two direct optimization ones, were used to
528 determine the values of the shape and scale parameters of a Weibull distribution function representing
529 the wind speeds organized in 20 classes. The direct optimization methods consist to minimize an
530 objective function which involves the squared differences between the observed and simulated
531 frequencies or probabilities, with respect to the two parameters of a Weibull function. The errors

532 between the observed and simulated wind speeds were lower using the direct optimization methods.
533 The Annual Energy Potential deduced from the values of the parameters of the Weibull function
534 simulating the wind speeds was significantly lower when considering the direct optimization
535 methods. A sensitivity analysis and a parametric study were conducted on this Annual Energy
536 Production with respect to the power output of the turbine and to the density of a Weibull function
537 representing the wind speed probabilities. For the wind directions, a superposition of two von Mises
538 distributions was applied with good agreement for each site. Here again, direct optimization methods
539 were applied to derive the parameters involved in this superposition of two von Mises distributions.
540 As soon as wind turbines will be installed in the three chosen sites, their behavior will be compared
541 with the simulations performed in the present study. Working in an Arctic region, icing and de-icing
542 phenomena surely will occur and should be taken into account, as they penalize the optimal behavior
543 of the wind turbines.

544

545 Funding. The authors did not receive support from any organization for the submitted work.

546 Conflict of interest. The authors have no competing interests to declare that are relevant to the content
547 of this article.

548

549 **References**

- 550 1. Weis, T.M., Ilinca, A.: Assessing the potential for a wind power incentive for remote villages
551 in Canada. *Energy Policy*. 38, 5504–5511 (2010). <https://doi.org/10.1016/j.enpol.2010.04.039>
552 2. Souba, F., Mendelson, P.B.: Chaninik Wind Group: Lessons learned beyond wind integration
553 for remote Alaska. *The Electricity Journal*. 31, 40–47 (2018).
554 <https://doi.org/10.1016/j.tej.2018.06.008>
555 3. Ghani, R., Kangash, A., Virk, M.S., Maryandyshev, P., Mustafa, M.: Wind energy at remote
556 islands in arctic region—A case study of Solovetsky islands. *Journal of Renewable and*
557 *Sustainable Energy*. 11, 053304 (2019). <https://doi.org/10.1063/1.5110756>
558 4. ERA5 hourly data on single levels from 1979 to present. Accessed October 12th, 2021.,
559 <https://cds.climate.copernicus.eu/cdsapp#!/dataset/reanalysis-era5-single-levels?tab=form>
560 5. Freitas de Andrade, C., Ferreira dos Santos, L., Silveira Macedo, M.V., Costa Rocha, P.A.,
561 Ferreira Gomes, F.: Four heuristic optimization algorithms applied to wind energy:
562 determination of Weibull curve parameters for three Brazilian sites. *Int J Energy Environ Eng.*
563 10, 1–12 (2019). <https://doi.org/10.1007/s40095-018-0285-5>

- 564 6. Kollu, R., Rayapudi, S., Narasimham, S., Pakkurthi, K.: Mixture probability distribution
565 functions to model wind speed distributions. *Int J Energy Environ Eng.* 3, 27 (2012).
566 <https://doi.org/10.1186/2251-6832-3-27>
- 567 7. Vestas: Vestas V90 wind turbine.
568 https://www.vestas.com/en/products/2%20mw%20platform/v90%202_0_mw#!. Accessed
569 October 5th, 2021,
570 https://www.vestas.com/en/products/2%20mw%20platform/v90%202_0_mw#!
- 571 8. International Electrotechnical Commission: Wind energy generation systems. Part 12-1.
572 (2017)
- 573 9. Khalid Saeed, M., Salam, A., Rehman, A.U., Abid Saeed, M.: Comparison of six different
574 methods of Weibull distribution for wind power assessment: A case study for a site in the
575 Northern region of Pakistan. *Sustainable Energy Technologies and Assessments.* 36, 100541
576 (2019). <https://doi.org/10.1016/j.seta.2019.100541>
- 577 10. Jung, C., Schindler, D.: The role of air density in wind energy assessment – A case study from
578 Germany. *Energy.* 171, 385–392 (2019). <https://doi.org/10.1016/j.energy.2019.01.041>
- 579 11. Masseran, N., Razali, A.M., Ibrahim, K., Latif, M.T.: Fitting a mixture of von Mises
580 distributions in order to model data on wind direction in Peninsular Malaysia. *Energy*
581 *Conversion and Management.* 72, 94–102 (2013).
582 <https://doi.org/10.1016/j.enconman.2012.11.025>
- 583 12. Diyoke, C.: A new approximate capacity factor method for matching wind turbines to a site:
584 case study of Humber region, UK. *Int J Energy Environ Eng.* 10, 451–462 (2019).
585 <https://doi.org/10.1007/s40095-019-00320-5>
- 586 13. Sunderland, K., Woolmington, T., Blackledge, J., Conlon, M.: Small wind turbines in
587 turbulent (urban) environments: A consideration of normal and Weibull distributions for
588 power prediction. *Journal of Wind Engineering and Industrial Aerodynamics.* 121, 70–81
589 (2013). <https://doi.org/10.1016/j.jweia.2013.08.001>
- 590 14. Quan, P., Leephakpreeda, T.: Assessment of wind energy potential for selecting wind turbines:
591 An application to Thailand. *Sustainable Energy Technologies and Assessments.* 11, 17–26
592 (2015). <https://doi.org/10.1016/j.seta.2015.05.002>
593